

Optothermal Study of Hydrogenated Amorphous Silicon-Sulfur Alloys

S.M. Al-Alawi

The optothermal properties of doped and undoped amorphous silicon-sulfur alloys have been studied using the optothermal transient emission radiometry (OTTER) technique. The optothermal decay signal was found to depend on the concentration of incorporated sulfur atoms in the material. The results have been correlated with the density of gap-state defects induced by sulfur atoms as determined from subgap absorption measurements. The OTTER technique has proved to be a viable alternative method for measuring the relative densities of defect states in the band gaps of amorphous silicon-sulfur alloys.

Keywords

hydrogenation, optic measurements, silicon alloys

1. Introduction

OPTOTHERMAL transient emission radiometry (OTTER) is a recently developed technique for studying changes in the optical absorption, thermal diffusivity, and related properties of opaque materials (Ref 1-5). This technique is nondestructive, noncontacting, and is applied to the free surface of the film. It uses a laser pulse to excite a small volume of the sample. The absorbed energy is dissipated rapidly in the form of heat, causing a steep rise in temperature at the surface, before a decay to ambient temperature. The changes in thermal infrared radiation from the material are sensed remotely using a high-speed infrared detector and recorded in a transient digitizer. Least-squares analysis of the optothermal decay curves can be used to deduce material properties. In this work, the OTTER technique has been employed to study the properties of doped and undoped amorphous silicon-sulfur alloys.

2. Theory

The time-dependent optothermal signal, $S(t)$, from a homogeneous semi-infinite sample with negligible scattering is given by (Ref 2, 4):

$$S(t) = \frac{K_1 \left[\sqrt{\tau_1} \exp(t/\tau_1) \operatorname{erfc} \left[\sqrt{t/\tau_1} \right] - \sqrt{\tau_2} \exp(t/\tau_2) \operatorname{erfc} \left[\sqrt{t/\tau_2} \right] \right]}{\tau_1 - \tau_2} \quad (\text{Eq 1})$$

where K_1 is a constant and

$$\tau_1 = \frac{1}{\alpha^2 D} \quad (\text{Eq 2})$$

S.M. Al-Alawi, Department of Physics, University of Bahrain, Isa Town, Bahrain.

and

$$\tau_2 = \frac{1}{\beta^2 D} \quad (\text{Eq 3})$$

where D is the thermal diffusivity of the sample, α is the absorbance for the excitation (i.e., $\alpha = \alpha[\lambda_{ex}]$), β is the absorbance for the emitted infrared radiation (Ref 2) (i.e., $\beta = \beta[\lambda_{em}]$), τ_1 and τ_2 are the optothermal decay times, t is time, and $\operatorname{erfc}(x) = 1 - \operatorname{erf}(x)$, where erf is the error function.

Attempts to use Eq 1 for decay curve analysis usually do not provide an accurate fit to experimental data because of the variation of the infrared absorbance with emission wavelength and because of the photothermal saturation (Ref 4, 5). Therefore, in this work an expression introduced by Imhof et al. (Ref 6) has been adopted to obtain a better fit to the experimental data. This expression is given by:

$$S(t) = K_2 A_1 \exp\left(\frac{t}{\tau_1}\right) \operatorname{erfc}\left(\sqrt{\frac{t}{\tau_1}}\right) + A_2 \exp\left(-\frac{t}{\tau_2}\right) \quad (\text{Eq 4})$$

where A_1 and A_2 are positive coefficients, proved suitable, erfc is a complementary error function, and K_2 is a constant. Equation 4 adequately represents the decay curves. The optothermal decay curves were analyzed using a nonlinear least-squares program.

3. Experimental Details

A schematic diagram of the conventional OTTER setup is shown in Fig. 1. A spectron Q-switched Nd:YAG laser and harmonic generator with output wavelengths of 1064, 532, 355, and 266 nm is used for excitation. The laser beam is directed onto the sample, forming an illuminated disk about 1 cm in diameter. The thermal infrared signal is collected by means of a $f/0.5$, 90° off-axis ellipsoidal mirror and is detected by a liquid-nitrogen-cooled cadmium-mercury-telluride (CMT) detector. The detected waveform is captured using a Datalab DL912 (Data*Lab, Inc., Boulder, CO) transient digitizer interfaced with a PC-AT computer for high-speed signal averaging of typically 100 excitation pulses. The average transient was processed following the procedure described in Ref 7.

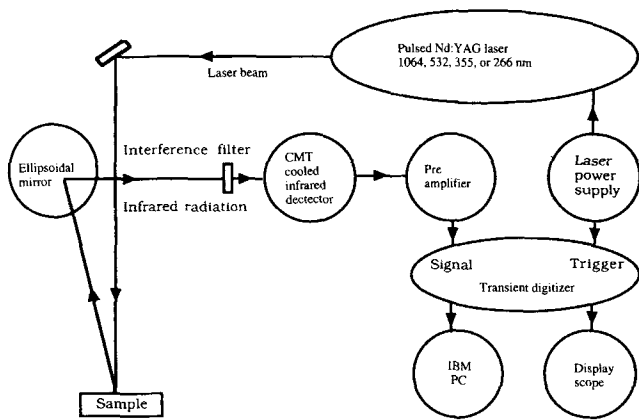


Fig. 1 Schematic of the OTTER setup

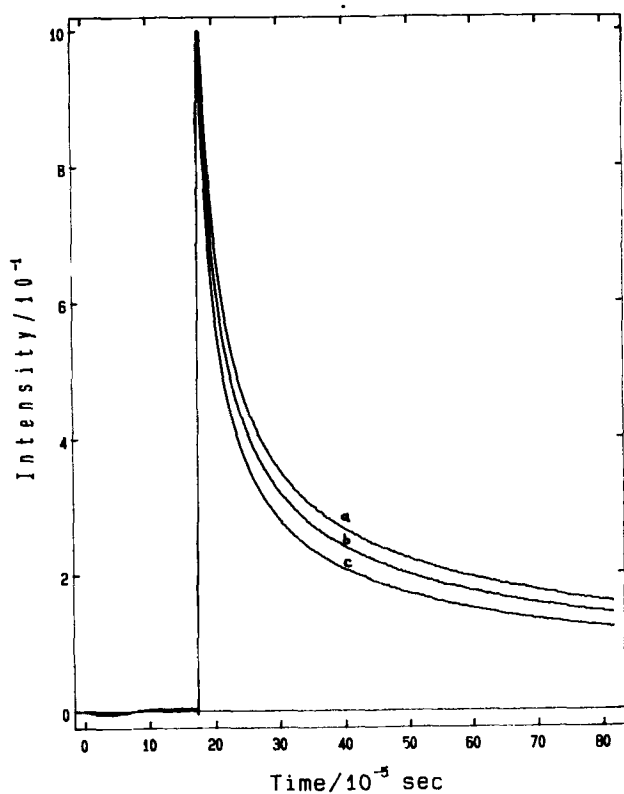


Fig. 2 Optothermal decay curves for undoped a-Si-S:H alloys. (a) $R_v = 0.4$. (b) $R_v = 0.6$. (c) $R_v = 0.8$

Hydrogenated amorphous silicon-sulfur alloy thin films were prepared by radiofrequency glow-discharge decomposition of 5% $\text{SiH}_4 + 95\% \text{He}$ and 2% $\text{H}_2\text{S} + 98\% \text{He}$ mixtures. Doped samples were prepared by addition of 0.1% $\text{PH}_3 + 99.9\% \text{He}$ to the gaseous mixture. Helium dilution of the reactant gases was employed for safety purposes. A capacitively coupled system supplied the radiofrequency power to the plasma. Films were deposited on Corning 7059 (Corning Inc., Corning, NY) glass. The process pressure was maintained at 40

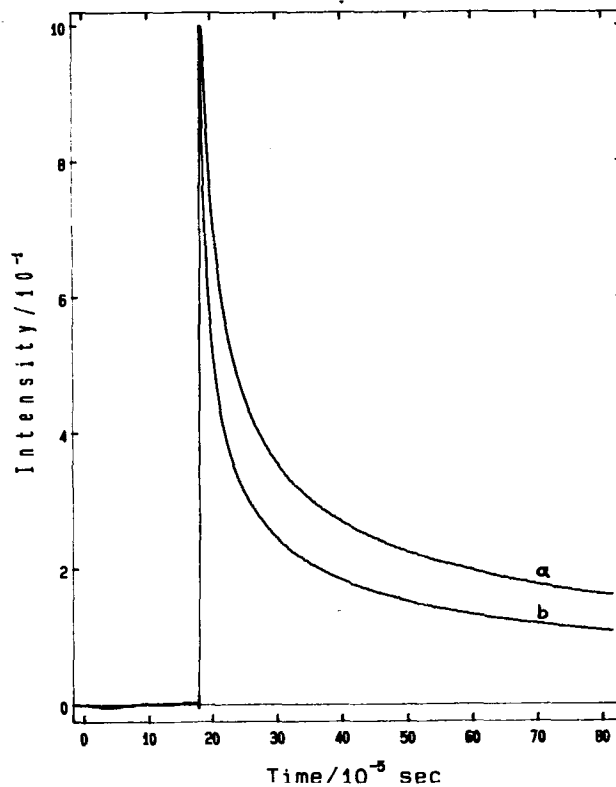


Fig. 3 Optothermal decay curves for phosphorus-doped a-Si:S:H alloys for $R_v = 0.6$. Flow rates of 0.1% $\text{PH}_3 + 99.9\% \text{He}$ gaseous mixture: (a) $10 \text{ cm}^3/\text{min}$; (b) $50 \text{ cm}^3/\text{min}$

Pa (0.3 torr), and the plasma power was kept constant at 20 W for different films. The power density in a 20 W plasma discharge is about $110 \text{ mW}/\text{cm}^2$. The total flow rate was kept at $35 \text{ cm}^3/\text{min}$. Samples were at a constant temperature of 270°C . Nondestructive optothermal measurements were carried out at room temperature. The deposition rate was found to be a function of the gas flow ratio, $R_v = (\text{H}_2\text{S})/(\text{SiH}_4)$.

4. Results and Discussion

Figures 2 and 3 show typical optothermal decay curves for undoped and phosphorus-doped amorphous silicon-sulfur alloys, respectively. The decays are characterized by a fast initial component, which is usually associated with a homogeneous composition (Ref 8). Table 1 summarizes the optothermal data obtained from least-squares analysis using Eq 4. Fitted decay times calculated from such analysis were found to vary from $56 \mu\text{s}$ for samples characterized by $R_v = 0.4$ to $118 \mu\text{s}$ for samples with $R_v = 0.8$. An important feature in Fig. 2 is that the incorporation of sulfur in the silicon matrix enhances the optothermal decay. Similarly, for identical sulfur content, the incorporation of phosphorus atoms induces a faster decay rate of the optothermal signal (Fig. 3).

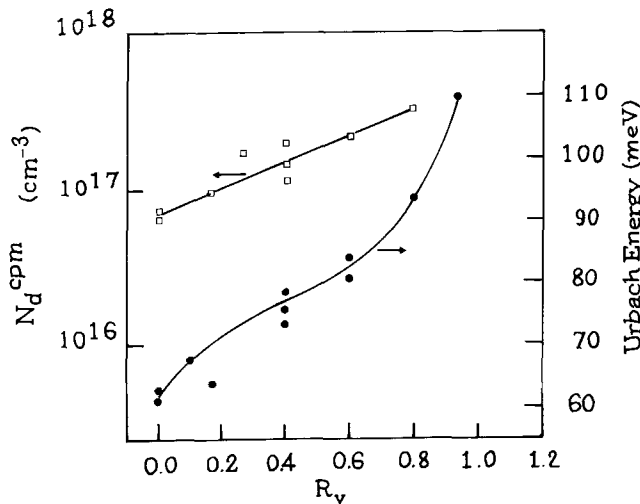
To elucidate the nature of this behavior, the compositional variation of the Urbach energy was determined from subgap absorption measurements. Photothermal deflection spectroscopy

Table 1 Optothermal data obtained from least-squares analysis using Eq 4

Urbach energy and defect density data were obtained from subgap absorption measurements using the CPM technique

Sample(a)	A_1	A_2	τ_1 , μs	τ_2 , μs	E_u , meV	N_d , cm^{-3}
S_1 (a)	1.96	0.037	13.77	118	77	2×10^{18}
S_2 (b)	1.98	0.050	10.22	76.5	85	4.8×10^{17}
S_3 (c)	2.02	0.046	7.32	56.3	94	9×10^{16}
P_1 (a)	2.09	0.013	11.65	7.51	...	3.2×10^{17}
P_2 (b)	2.21	0.032	3.82	233.7	...	8.3×10^{16}

(a) The indicators (a), (b), and (c) refer to the curves shown in Fig. 2 and 3.

**Fig. 4** Compositional dependence of defect density and Urbach energy for undoped a-Si:H alloys

copy (PDS) and constant photocurrent method (CPM) spectra were analyzed to obtain the Urbach energy (E_u) and the deep defect density (N_d) (Ref 9). The latter was determined from the subgap defect absorption shoulder using the same factor as that used from a-Si:H (Ref 10). Figure 4 summarizes the results of this analysis. In hydrogenated amorphous silicon-sulfur alloys, E_u rises from 62 to 110 meV as R_v increases from 0 to 0.93. For the same change in R_v , N_d increases from $5 \times 10^{16} \text{ cm}^{-3}$ in the unalloyed material to about $5 \times 10^{17} \text{ cm}^{-3}$ for $R_v = 0.93$. These data are summarized in Table 1.

The values of N_d and E_u obtained for the experimental samples are in good agreement with reported data on similar materials, such as a-Si:H (Ref 9) and a-Si:C:H (Ref 11). The data given in Table 1, including τ_1 , τ_2 , A_1 , and A_2 , are found to be highly reproducible for various compositions. Values for E_u and N_d are from CPM and PDS and are quite accurate to within $\pm 5 \text{ meV}$ for E_u and $\pm 20\%$ for N_d .

The above analysis suggests a correlation between the defect states in the band gap of hydrogenated amorphous silicon-sulfur alloys and the decay rate of the optothermal signal. Increasing the sulfur content results in a higher density of defect states, which provides a nonradiative transition path to the excited carriers and consequently a faster optothermal decay time.

Phosphorus-doped samples show a similar trend. The higher the phosphorus concentration, the faster the decay rate of the optothermal signal. Previous work on doped amorphous silicon has shown that phosphorus introduces an additional distribution of defect states in the vicinity of the conduction band edge (Ref 12).

5. Conclusions

Optothermal transient emission radiometry is a viable technique for characterizing relative changes in defect density in amorphous silicon-sulfur alloys with changing element composition. This technique can also be used to characterize defects in other amorphous networks.

Acknowledgments

The author would like to thank Dr. S. Al-Dallal, Dr. Samer Aljishi, and Dr. Mahmood Hammam for useful discussions, as well as Dr. R.E. Imhof and Dr. R.M.S. Bindra for providing the facilities for performing the optothermal measurements.

References

1. A.C. Tam and B. Sullivan, Remote Sensing Applications of Pulsed Photothermal Radiometry, *Appl. Phys. Lett.*, Vol 43, 1983, p 333-335
2. R.E. Imhof, D.J.S. Birch, F.R. Thornely, J.R. Gilchrist, and T.A. Strivens, Optothermal Transient Emission Radiometry, *J. Phys. E: Sci. Instrum.*, Vol 17, 1984, p 521-525
3. R.E. Imhof, D.J.S. Birch, F.R. Thornely, S.M. Al-Alawi, and J.R. Gilchrist, in *The Influence of New Technology in Medical Practice*, J.P. Paul, A.B. McCrudden, and P.W. Schuetz, Ed., Macmillan, 1988
4. R.E. Imhof, C.J. Whitters, D.J.S. Birch, and F.R. Thornely, New Opto-Thermal Radiometry Technique Using Wavelength-Selection Detection, *J. Phys. E: Sci. Instrum.*, Vol 21, 1988, p 115-117
5. R.E. Imhof, C.J. Whitters, and D.J.S. Birch, Time-Domain Optothermal Spectro-Radiometry, *Photoacoustic and Photothermal Phenomena II*, J.C. Murphy, J.W. MacLachlan-Spicer, L. Aamodt, and B.S.H. Royce, Ed., Springer-Verlag, Berlin, 1990, p 46-54
6. R.E. Imhof, F.R. Thornely, J.R. Gilchrist, and D.J.S. Birch, Optothermal Study of the Melting Transition of Benzophenone, *Appl. Phys. B*, Vol 43, 1987, p 23-28
7. R.E. Imhof, C.W. Whitters, and D.J.S. Birch, Opto-Thermal In-Vivo Monitoring of Structural Breakdown of an Emulsion Sunscreen on Skin, *Clin. Mater.*, Vol 5, 1990, p 271-278

8. P.H. Wilson, R.E. Imhof, D.J.S. Birch, and J.F. Webb, Opto-Thermal Investigation of Dichroic Materials, *Photoacoustic and Photothermal Phenomena II*, J.C. Murphy, J.W. Maclachlan-Spicer, L. Aamodt, and B.S.H. Royce, Ed., Springer-Verlag, Berlin, 1990, p 322-325
9. S.M. Al-Alawi, H. Hammam, S. Aljishi, H.S. Al-Alawi, and S. Al-Dallal, Novel Non-Stoichiometric Amorphous Silicon-Chalcogen Semiconductor Alloys, *The Physics of Non-Crystalline Solids*, L.D. Pye, W.C. LaCourse, and H.J. Stevens, Ed., Taylor & Francis, London, 1992, p 218
10. Z.E. Smith, V. Chu, K. Shepared, S. Aljishi, K. Kolodzey, T.L. Chu, and S. Wagner, Photothermal and Photoconductive Determination of Surface and Bulk Defect Densities in Amorphous Silicon Films, *Appl. Phys. Lett.*, Vol 50, 1987, p 1521
11. S.H. Baker, W.E. Spear, and R.A.G. Gibson, Electronic and Optical Properties of a-Si_{1-x}C_x Films Prepared from a H₂-diluted Mixture of SiH₄ and CH₄, *Philos. Mag. B*, Vol 62, 1990, p 213-223
12. D.A. Anderson and W. Paul, Transport Properties of a-Si:H Alloys by r.f. Sputtering, *Philos. Mag. B*, Vol 45, 1982, p 1-23